Biochemistry and Biophysics Reports 27 (2021) 101043

Contents lists available at ScienceDirect

Biochemistry and Biophysics Reports

journal homepage: www.elsevier.com/locate/bbrep

In silico investigation of pro-arrhythmic effects of azithromycin on the human ventricle

Yizhou Liu [a], Rai Zhang [b], Jules C. Hancox [a,c,**], Henggui Zhang [a,d,e,*]

[a] Biological Physics Group, School of Physics and Astronomy, University of Manchester, Manchester, United Kingdom
[b] School of Civil, Aerospace and Mechanical Engineering, University of Bristol, United Kingdom
[c] School of Physiology, Pharmacology and Neuroscience, Cardiovascular Research Laboratories, School of Medical Sciences, University of Bristol, Bristol, United Kingdom
[d] Qingdao National Laboratory for Marine Science and Technology, Qingdao, China
[e] Key Laboratory of Medical Electrophysiology of Ministry of Education and Medical Electrophysiological Key Laboratory of Sichuan Province, Institute of Cardiovascular Research, Southwest Medical University, Luzhou, China

ARTICLE INFO

Keywords:
Azithromycin
Arrhythmia
Cardiac modelling
Human ventricle
COVID-19

ABSTRACT

The macrolide antibiotic azithromycin (AZM) is widely used for respiratory infections and has been suggested to be a possible treatment for the Coronavirus Disease of 2019 (COVID-19). However, AZM-associated QT interval prolongation and arrhythmias have been reported. Integrated mechanistic information on AZM actions on human ventricular excitation and conduction is lacking. Therefore, this study was undertaken to investigate the actions of AZM on ventricular cell and tissue electrical activity. The O'Hara- Virag-Varro-Rudy dynamic (ORd) model of human ventricular cells was modified to incorporate experimental data on the concentration-dependent actions of AZM on multiple ion channels, including I_{Na}, I_{CaL}, I_{Kr}, I_{Ks}, I_{K1} and I_{NaL} in both acute and chronic exposure conditions. In the single cell model, AZM prolonged the action potential duration (APD) in a concentration-dependent manner, which was predominantly attributable to I_{Kr} reduction in the acute condition and potentiated I_{NaL} in the chronic condition. High concentrations of AZM also increased action potential (AP) triangulation (determined as an increased difference between APD_{30} and APD_{90}) which is a marker of arrhythmia risk. In the chronic condition, the potentiated I_{NaL} caused a modest intracellular Na^+ concentration accumulation at fast pacing rates. At the 1D tissue level, the AZM-prolonged APD at the cellular level was reflected by an increased QT interval in the simulated pseudo-ECG, consistent with clinical observations. Additionally, AZM reduced the conduction velocity (CV) of APs in the acute condition due to a reduced I_{Na}, and it augmented the transmural APD dispersion of the ventricular tissue, which is also pro-arrhythmic. Such actions were markedly augmented when the effects of chronic exposure of AZM were also considered, or with additional I_{Kr} block, as may occur with concurrent use of other medications. This study provides insights into the ionic mechanisms by which high concentrations of AZM may modulate ventricular electrophysiology and susceptibility to arrhythmia.

1. Introduction

Azithromycin is a macrolide antibiotic used to treat a range of bacterial infections, including respiratory conditions such as sinusitis, bronchitis and pneumonia [1]. It is also used to prevent bacterial infections in people with weakened immune systems [1]. Recently, azithromycin (AZM) in combination with chloroquine (CQ)/hydroxychloroquine (HCQ) has been studied as a potential treatment for coronavirus disease of 2019 (COVID-19) caused by the SARS-CoV-2 virus [2]. Some observational studies have suggested clinical benefits of this combination in COVID-19 (e.g. [3,4]). Data from *in vitro* experiments are suggestive that AZM may modulate the pH of endosomes and *trans*-Golgi network [5], which provides a plausible mechanism for activity against SARS-Cov-2 [2,5]. However, there are concerns about the efficacy and safety in the use of CQ/HCQ for COVID-19 (e.g. [6]), with a recent randomised, open-label trial involving hospitalised patients unable to confirm a benefit of HCQ, with or without azithromycin for in-hospital outcomes and revealing an

* Corresponding author. Biological Physics Group, School of Physics and Astronomy, University of Manchester, Manchester, United Kingdom.
** Corresponding author. School of Physiology, Pharmacology and Neuroscience, Cardiovascular Research Laboratories, School of Medical Sciences, University of Bristol, Bristol, United Kingdom.
E-mail addresses: jules.hancox@bristol.ac.uk (J.C. Hancox), henggui.zhang@manchester.ac.uk (H. Zhang).

https://doi.org/10.1016/j.bbrep.2021.101043
Received 27 August 2020; Received in revised form 8 April 2021; Accepted 1 June 2021

increased frequency of QT interval prolongation in patients receiving HCQ, alone or with azithromycin [7].

The macrolide agents erythromycin and clarithromycin have been considered to have a greater risk of cardiotoxicity (linked to repolarization abnormality and ventricular arrhythmia) than has AZM [8]. In preclinical studies, acutely applied AZM has been reported to be a weak inhibitor of the hERG potassium channel (pharmacological blockade of which is strongly implicated in drug-induced QT prolongation and *Torsades de Pointes* (TdP) [9]) and not to cause QT_c interval prolongation in anaesthetized dogs [10]. Comparison of the acute effects of erythromycin, clarithromycin and AZM on perfused rabbit hearts has suggested that AZM did not share proarrhythmic effects of the other two macrolides [11]. On the other hand, a small absolute increase in cardiovascular deaths has been reported in patients during five days of azithromycin treatment [12]. Analysis of case reports in which AZM has been associated with QT interval prolongation/TdP arrhythmia suggests that this occurs in the presence of additional risk factors [13]. Cases of polymorphic ventricular tachycardia without QT prolongation have also been reported for AZM [14,15]. AZM exerts modest inhibitory effects on several cardiac ion channels; notably a recent study has shown that acute azithromycin decreases cardiac fast Na current, I_{Na}, whilst chronic exposure increases both peak I_{Na} and the late component of Na current, I_{NaL} [15]. Acute application of the drug to mice was found to produce marked changes to PR, QRS, and QT intervals, consistent with multi-channel effects of the drug, whilst the chronic Na^+ channel effects raised the possibility of altered Na^+ loading and associated pro-arrhythmia [15]. Overall ventricular repolarization mechanisms differ between mice and humans [16], however, and the study of the consequences of AZM actions on cardiac ion channels would thus best be undertaken using human cardiac preparations. Therefore, this study employed biophysically accurate human ventricular cell and tissue models, in order to evaluate effects of AZM on human ventricular electrophysiology. Our results indicate that at higher concentrations, AZM produces changes to action potential conduction and repolarization that may increase ventricular arrhythmia risk.

2. Materials and methods

The O'Hara-Virag-Varro-Rudy dynamic (ORd) human ventricular action potential (AP) model was used [17]. This model has been validated by extensive experimental data, and can reproduce a large range of physiological behaviours [17]. Recently, the ORd model has been further improved by Whittaker et al. [18] by replacing the fast sodium current formulations by those from the Luo-Rudy model [19] for simulating stable AP propagation in the tissue level, and a Markov chain model for the rapid delayed rectifier potassium current, I_{Kr} [18,20]. In this study, we adopted the modified version of the ORd model [18] with a replaced fast sodium current formulation from the Luo-Rudy model [19] for the human atrial cells for maintaining the intracellular Na^+ concentration homeostasis over a long simulation period (>200 s), pacing at 1 Hz. To determine whether or not our simulation results were model-dependent, the most-updated model of human ventricular AP developed by Tomek et al. [21] was also implemented for single cell simulations.

To simulate the acute and chronic effects of azithromycin, experimental data on the concentration-dependent fractional block and potentiation of ion channel currents from the study of Yang et al. [15] were incorporated into the model. These experimental data were obtained by application of the whole-cell patch clamp technique to heterologously expressed ion channels or to cardiomyocytes, to evaluate the concentration-dependent inhibition of ion channel currents on acute exposure to AZM, including: the fast Na^+ current (I_{Na}), L-type Ca^{2+} current (I_{CaL}), rapid delayed rectifier K^+ current (I_{Kr}), slow delayed rectifier K^+ current (I_{Ks}) and inward rectifier K^+ current (I_{K1}); as well as the dose-dependent potentiation of I_{Na} and late Na current (I_{NaL}) during the chronic exposure of the channels to the drug (chronically exposed to azithromycin for 24 h). To simulate the combined action of acute and chronic effects of AZM, the rapid block of I_{Na} under acute exposure was replaced by the potentiation of I_{Na} and I_{NaL}, whilst AZM's actions on other ion channels remained as in the acute case. For treatment of Covid-19, AZM has been suggested to be used with HCQ, a potassium channel blocker. Therefore, further simulation scenarios were considered in which an additional 25% or 50% I_{Kr} inhibition was incorporated, to mimic co-administration of AZM with (a) drug(s) with I_{Kr} blocking properties. Details of AZM effects on ion channels for acute and chronic conditions are documented in Supplementary Table S1.

In single cell simulations, the model was paced with a series of 500 stimuli with an amplitude of −20 pA/pF and duration of 2.0 ms at 1 Hz to reach the steady-state. The AP and corresponding ion channel current traces were recorded for analysis. The action potential duration (APD) restitution was also measured using an S1–S2 protocol.

To simulate ventricular excitation wave conduction, a 1D tissue model was constructed based on the monodomain equation of cardiac tissue,

$$\frac{\partial V_m}{\partial t} = \nabla \cdot D \nabla V_m - \frac{I_{tot}}{C_m}$$

where V_m is the membrane potential, t the time, C_m the cell capacitance, I_{tot} the total cell mebrane corrent, and D the diffusion coefficient. In simulations, the 1D model had a length of 15 mm, which was discretised into a strand of 100 nodes with a spatial resolution of 0.15 mm, consisting of 25 nodes for representing endocardial cells (ENDO), 35 nodes for middle cells (MCELL) and 40 nodes for epicardial cells (EPI). The length and composition of the 1D strand were consistent with our previous studies for normal human transmural ventricular tissue. The diffusion coefficient 'D' was set to 0.1171 mm^2/ms throughout the strand except for the EPI-MCELL border where there was a five-fold decrease in the diffusion coefficient as 0.02342 mm^2/ms, which gave a general conduction velocity (CV) across the strand at 61 cm/s, matching to experimental observations.

The pseudo-ECG (pECG) was computed using the method proposed by Gima and Rudy [18]. The unipolar potentials at position (x', y', z'), Φ (x',y',z'), is given by:

$$\Phi(x', y', z') = \int (-\nabla V_m) \cdot \left(\nabla \frac{1}{r} \right) d\Omega$$

$$r = \sqrt{(x - x')^2 + (y - y')^2 + (z - z')^2},$$

where r is the distance from a source point (x,y,z) to a field point (x',y', z') (about 2 cm from the epicardial end of the strand), and Ω is the domain of integration covering the whole 1D strand.

Using the 1D strand model, we computed the effects of the AZM on the conduction properties of electrical excitation waves, including the CV, the QT interval of pECG, transmural APD_{90} dispersion using the same method as in our previous studies.

3. Results and discussion

Fig. 1 shows the effect of acute action of AZM on APs evoked at 1 Hz from the ENDO ventricular cell model together with the drug's effects on key underlying ion channel currents. At a concentration of 1 μM, AZM produced little effect on AP parameters or underlying currents. However, at 50 and 100 μM AZM, concentration-dependent prolongation of AP duration (APD_{90}) and reduction of maximum upstroke velocity (MUV) were observed. These effects were linked to underlying reductions to I_{Kr}, I_{K1} and I_{Ks} (Fig. 1D–F) at these higher concentrations, whilst reduction in rapid I_{Na} (Fig. 1B) accounted for the reduction in upstroke velocity. A small reduction in $[Na^+]_i$, associated with the reduced I_{Na} (Fig. 1B) and I_{CaL} reduction (Fig. 1C), which potentially could influence Ca^{2+} cycling, was also seen. Similar results on the effects

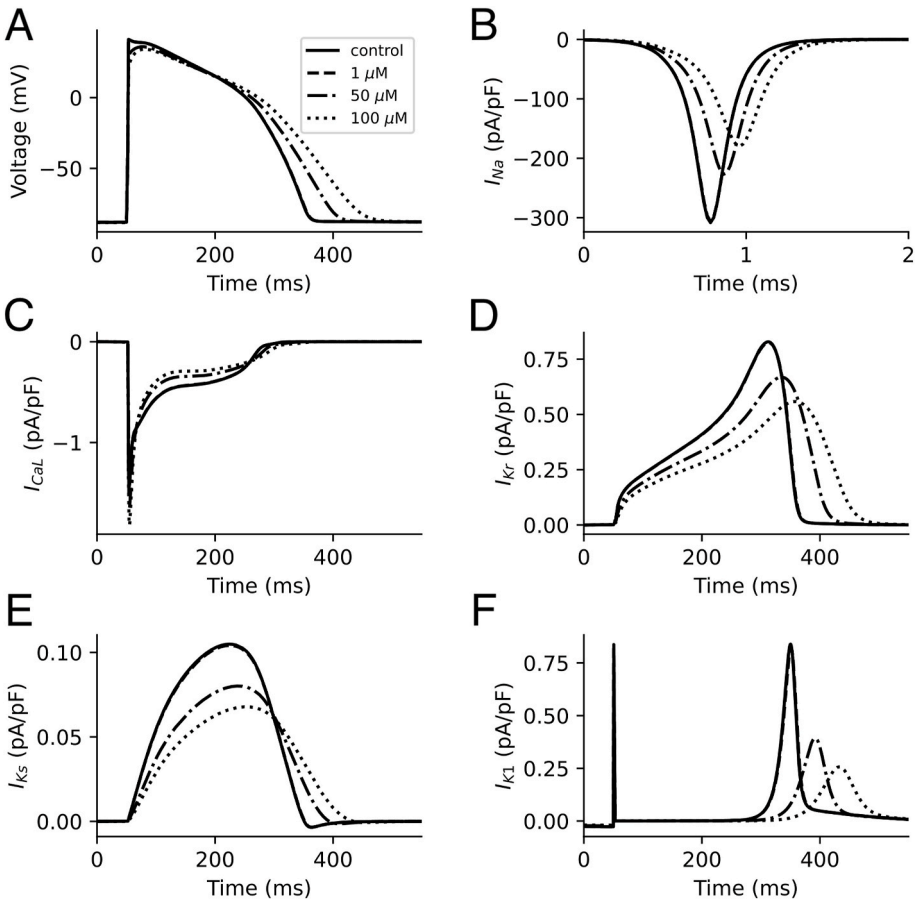

Fig. 1. Simulation of acute effects of azithromycin on ventricular single cell action potentials and underlying relevant ion channel current traces. (**A**) Endocardial action potential (AP) at 1 Hz under control, 1 μM azithromycin, 50 μM azithromycin, 100 μM azithromycin conditions. Corresponding current profiles for I_{Na} **(B)**, I_{CaL} **(C)**, I_{Kr} **(D)**, I_{K1} **(E)** and I_{Ks} **(F)**.

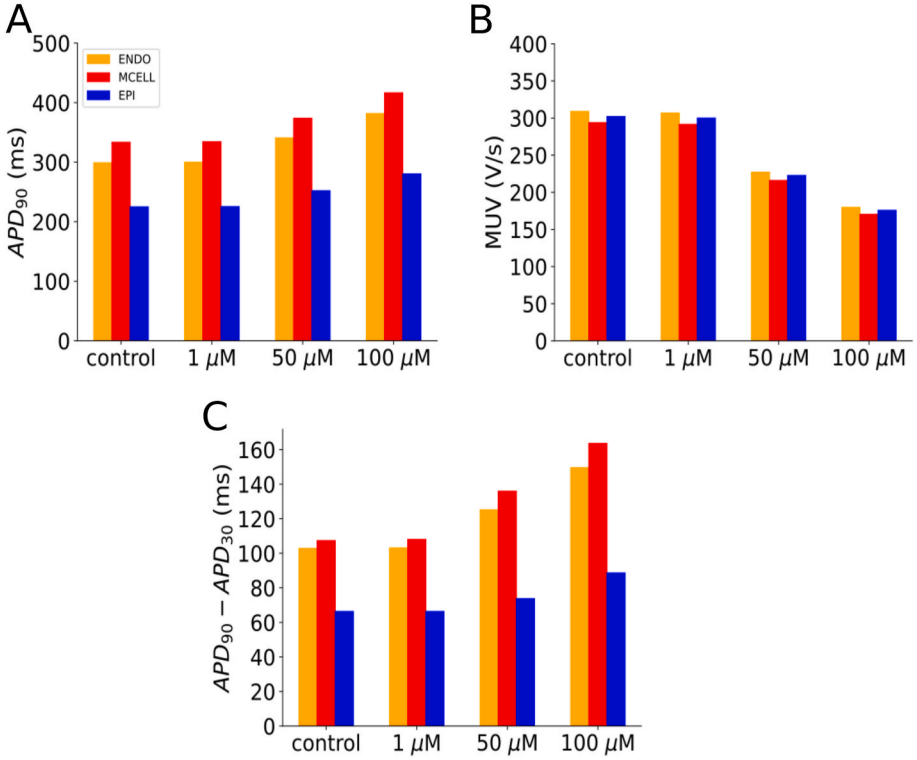

Fig. 2. Computed characteristics of APs from ENDO, MCELL and EPI cell models in control and different AZM concentrations. The concentration-dependence of the single cell AP duration at 90% repolarization (APD_{90}) and maximum upstroke velocity (MUV) for endocardial cells (orange bar), middle cells (red bar) and epicardial cells (blue bar) are shown in **(A, B)**, respectively. The difference of between single cell AP duration at 30% repolarization (APD_{30}) and APD_{90} is illustrated in **(C)**. **(For interpretation of the references to colour in this figure legend, the reader is referred to the Web version of this article.)**

of acute action of AZM on APs were also observed in the Tomek et al. [21] model as shown in Fig. S1 in the Online Supplemental Materials.

Fig. 2 summarizes graphically the computed APD_{90} (Fig. 2A), MUV (Fig. 2B) and the difference between APD_{30} and APD_{90}, as an index of AP triangulation (Fig. 2C) for ENDO, MCELL and EPI cells in control and with three different acutely applied concentrations of AZM. These plots show relatively little effect of 1 μM AZM and marked concentration-dependent effects of 50 and 100 μM AZM. Although similar consequences were observed for all of the three different cell types, the concentration-dependent changes to the characteristics of the MCELL were greater than those seen in the ENDO and EPI cells, consistent with an augmented transmural heterogeneity across the ventricular wall. The effect of AZM on the rate dependence of APD_{90} is shown in Fig. S2, which shows that AZM had a greater APD prolongation at the larger basic cycle lengths (BCLs). Notably, APD triangulation is a marker of arrhythmia risk [22] and not only was this increased for all cell types by 50 and 100 μM AZM, but the EPI-MCELL difference in triangulation was increased by the drug.

Fig. 3 compares the simulated APs (Fig. 3A) from the ENDO cell model under control, actions of AZM (acute), AZM with additional 25% I_{Kr} block (to mimic co-application of AZM with another I_{Kr} blocking drug) and with the incorporation of chronic effects of AZM to augment peak I_{Na} and I_{NaL} [15]. In the figure, results from a representative AZM concentration at 50 μM are shown; effects of further AZM concentrations of APs can be found in Fig. S3. When combined with a 25% I_{Kr} block, AZM further prolonged the APD and reduced the AP overshoot (Fig. 3A). When a combined action of acute and chronic effects of AZM was considered, the APD was even further prolonged, but the AP overshoot reduction was reversed, resulting in an AP overshoot that was comparable to that seen in the control condition. These changes in AP characteristics were attributable to the integrated action of the underlying ion channel currents, including I_{Na} (Fig. 3B), I_{CaL} (Fig. 3C), I_{Kr} (Fig. 3D), I_{K1} (Fig. 3E), I_{Ks} (Fig. 3F) and I_{NaL} (Fig. 3G). As summarized in Table 1, effects of AZM on APD_{90} were further exacerbated when the extent of concomitant I_{Kr} inhibition was increased from 25 to 50%.

Fig. 4A–C shows the simulated effect of acute AZM from the 1D strand model on the CV of ventricular excitation waves, pseudo ECG and the maximal spatial gradient of APD_{90} across the 1D strand. AZM decreased CV in the 1D strand (Fig. 4A), which was attributable to the inhibitory action of AZM on fast I_{Na} that resulted in a reduced MUV. The alteration to CV was negligible with 1 μM AZM, but noticeable at the higher concentrations tested (further details are given in Table 1), arising from the concentration-dependent reduction of I_{Na}. Further results of measured CVs at 1 Hz in different conditions are given in Table 1. Note that in the chronic condition, AZM increased rather than decreased the CV (Table 1) as chronic AZM increased rather than decreased I_{Na}. The AZM-induced changes to peak I_{Na} were also associated with small changes to QRS width on the pseudo ECG, with acute exposure

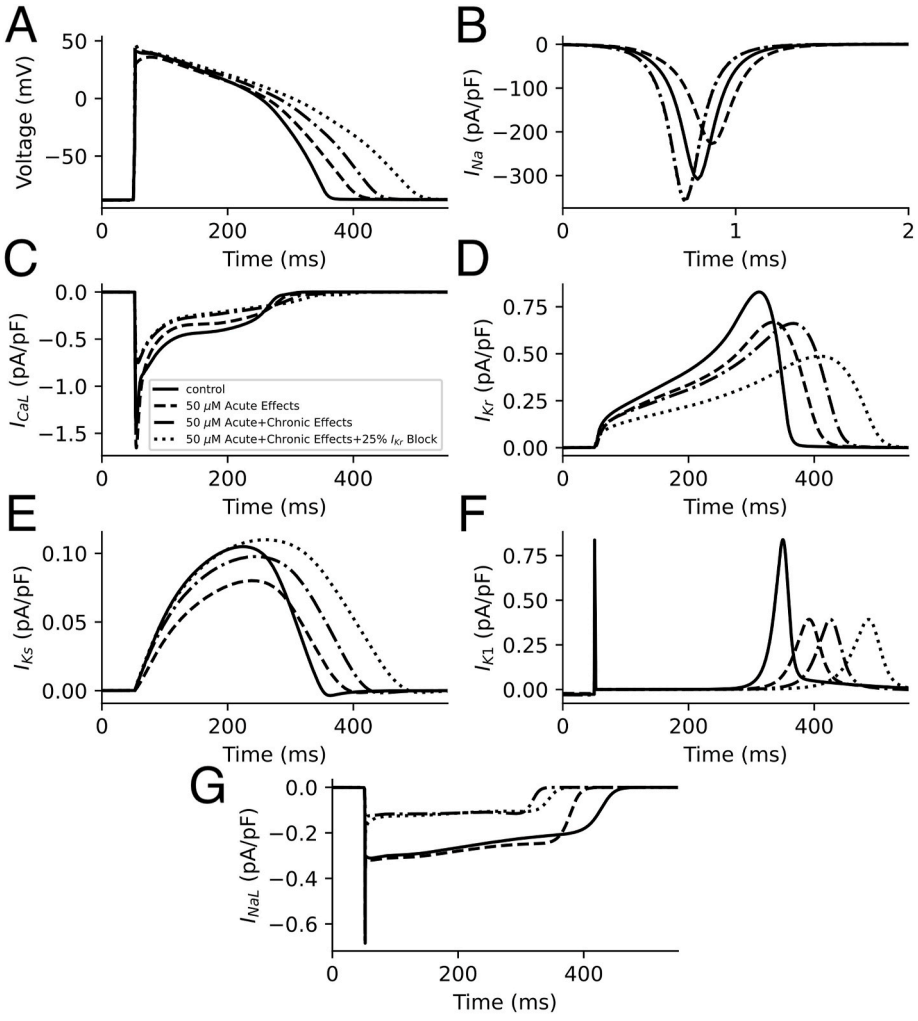

Fig. 3. Action of acute, chronic azithromycin with additional I_{Kr} block on ventricular action potentials and current traces. (A) Endocardial action potential (AP) at 1 Hz under control, 50 μM azithromycin acute effects, 50 μM azithromycin acute effects + 25% I_{Kr} block, 50 μM azithromycin acute effects + 50 μM azithromycin chronic effects + 25% I_{Kr} block conditions. Corresponding current profiles for I_{Na} **(B)**, I_{CaL} **(C)**, I_{Kr} **(D)**, I_{K1} **(E)**, I_{Ks} **(F)** and I_{NaL} **(G)**.

Table 1
Summary of both acute and chronic effects of azithromycin in single cell and 1D simulation. Comparison of action potential duration at 90% repolarization (APD_{90}), maximum upstroke velocity (MUV) in single cell model, conduction velocity (CV), QT interval, QRS interval and distance between Twave Peak and Twave End in 1D pseudo ECG are listed.

	APD_{90} (ms)	MUV (V/s)	CV (cm/s)	QT Interval (ms)	QRS Interval (ms)	Twave Peak - Twave End (ms)
Control	298.9	308.9	60.8	399	26	78
Acute Effects						
1 μM	299.8	306.7	60.3	400	26	79
50 μM	340.7	227.1	53.6	454	29	100
100 μM	381.6	179.7	48.4	506	32	121
Chronic Effects						
1 μM	299.6	313.1	57.8	341	27	71
50 μM	320.6	472.8	69.2	366	23	79
100 μM	356.2	590.5	76.0	392	22	88
Acute Effects + Chronic Effects						
1 μM	300.5	311.2	57.7	342	27	72
50 μM	373.1	355.7	61.5	425	25	97
100 μM	467.6	367.5	62.3	513	25	126
Acute Effects + Chronic Effects + 25% I_{Kr} Block						
1 μM	345.2	311.5	57.7	391	27	75
50 μM	433.3	357.0	61.5	487	25	101
100 μM	537.0	368.2	62.3	582	25	131
Acute Effects + Chronic Effects + 50% I_{Kr} Block						
1 μM	410.8	312.0	57.8	464	27	78
50 μM	523.7	357.8	61.6	577	25	105
100 μM	637.0	368.8	62.5	683	25	136

increasing and chronic exposure narrowing QRS width (see Table 1). QRS widening on acute AZM administration is consistent with prior murine data obtained with intraperitoneal or oral AZM administration [15].

Strikingly, both acute and chronic exposure to AZM prolonged the QT interval of the pseudo ECG. Fig. 4B shows effects of acute AZM. 1 μM AZM produced virtually no change to the QT interval, whilst at 50 and 100 μM, measurable QT prolongation was observed. These observations indicate that the drug's inhibitory effects on I_{Kr} and other K^+ currents prevailed over the modest I_{CaL} inhibition produced by the drug. This effect was exacerbated by combining AZM with synergistic I_{Kr} block (to mimic co-application of another I_{Kr} inhibitor) and was also augmented when the inhibitory effects of AZM on K^+ currents were combined with increased I_{NaL} produced by chronic AZM exposure (Table 1). The gradient of APD_{90} dispersion, measured at the middle point of the 1D strand, was increased by acute AZM (at 50 and 100 μM; Fig. 4C) and this too was exacerbated in chronic AZM conditions or simulated application of additional I_{Kr} block (Table 1). This is an important observation as increased T_{peak}-T_{end} has been proposed to be a strong indicator of propensity towards TdP arrhythmia in patients with drug-induced LQTS [23].

As chronic Na^+ channel effects of AZM have been suggested potentially to influence arrhythmia susceptibility via increased Na^+ loading, consequent to augmented I_{NaL} [15], we investigated this. Fig. 4D shows $[Na^+]_i$ at quasi-steady-state in control and chronic AZM conditions under which AZM had augmented I_{NaL}. At a stimulation frequency of 1 Hz, a modest increase in $[Na^+]_i$ was observed with chronic 50 or 100 μM AZM exposure. When the stimulation frequency was increased to 2 Hz, the increase of $[Na^+]_i$ was greater. Such effects were not seen with acute AZM exposure (data not shown).

The results of this study are consistent with prior observations of APD and QT interval prolongation/TdP with AZM [13,24–27]. A significant APD_{90} prolongation with 830 mg/L AZM exposure (from control ~435 ms–~540 ms) was previously observed for APs recorded from guinea pig left ventricular myocytes [27]. Similar results were obtained using the monophasic action potential (MAP) recording/pacing combination catheter, which was positioned at the right ventricle in beagle dogs [28]. For human subjects, a recent analysis of the World Health Organization VigiBase pharmacovigilance database found significant reporting of QT prolongation/ventricular tachycardia (including TdP)

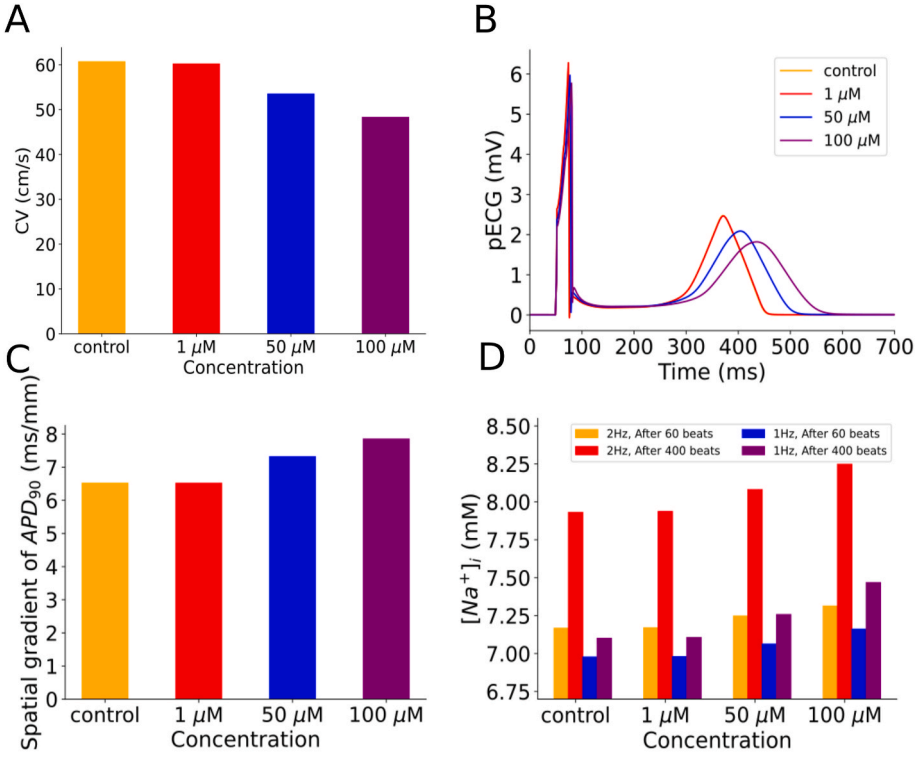

Fig. 4. 1D tissue modelling of acute effects of AZM and Na $^+$ overloading simulations. (A) Conduction velocity (CV). **(B)** Pseudo ECG traces. **(C)** Spatial gradient of action potential duration at 90% repolarization (APD_{90}) at the midpoint of the strand are shown respectively. **(D)** The intracellular $[Na^+]_i$ in control and the chronic AZM condition at different AZM concentrations. Results were computed from the ENDO cell model paced at 1 and 2 Hz.

for each of AZM and HCQ monotherapy. In the analysis, AZM showed a higher signal for potentially lethal events than HCQ. Evidence for a stronger effect of the drugs in combination was also presented [26]. Our results show both ventricular AP triangulation and augmented QT dispersion with AZM, which are proarrhythmic markers. Our findings also indicate that the effects of AZM on ventricular repolarization are exacerbated in the presence of additional I_{Kr} block. CQ is a well-known I_{Kr}/hERG blocker [29,30] and our results urge caution in combining AZM with other agents with I_{Kr}-blocking propensity. Indeed, narrative analysis of case reports has previously reported that QT interval prolongation/TdP with AZM were observed when other risk factors were present [13]. The presence of serious illness and concomitant presence of additional I_{Kr} blockade are likely such factors and, collectively, may explain the increased risk of QT prolongation or arrhythmia seen in hospitalized COVID-19 patients treated with CQ/HCQ and AZM [6,7,31]. It has been proposed that increased I_{Na}/I_{NaL} due to chronic AZM administration promotes Na^+ loading, which in turn may dysregulate intracellular Ca^{2+} and promote arrhythmogenesis [15]. Our simulations support the ability of chronic, high concentrations of AZM to increase $[Na^+]_i$; although the increase was modest (<0.5 mM at the higher rate studied), it led to a reduction of 1 mV in the Nernst potential for sodium.

In healthy subjects receiving 500 mg/day of AZM over three days peak plasma concentrations of 0.4 μg/ml (0.53 μM) have been reported [32]. In preclinical studies, intravenous AZM up to peak plasma concentrations of 20.8 μg/ml (~27.8 μM) did not prolong the QT_c interval of AV-blocked dogs [10], whilst in a separate study modest prolongation of canine Purkinje fibre APs was seen at 53.4 μM AZM and no significant prolongation at 0.53 μM [33]. Thus, if plasma/extracellular AZM concentrations alone are considered it is difficult to understand how AZM could exert significant effects on ventricular repolarization. However, Yang et al. have suggested that plasma AZM concentrations may be misleading, noting that marked tissue AZM accumulation can occur [15]. Consistent with this, accumulation of AZM in liver, spleen and heart of AZM-treated mice to levels 25-200-fold concurrent serum levels has been reported [34]. Our simulations showed no significant effect of AZM at 1 μM, with clear effects at 50 and 100 μM. Such drug concentrations are not representative of clinical plasma levels, but are consistent with those that could be achieved with intracellular AZM accumulation.

Our tissue simulations were limited to an idealized 1D strand and it is possible that the use of 2D or 3D tissue models, particularly those incorporating a realistic ventricle geometry might provide further insights into AZM-provoked arrhythmia. Similarly, the present study has not considered how autonomic nervous modulation may influence the effects of AZM. Model specificity of results is possible, but simulated effects of acute AZM on APs by using a recently-updated model of human ventricular AP [21] showed qualitatively similar results to those presented here (Fig. S1), suggesting that the observed action of acute AZM on APs at the single cell level was independent of model selection (i.e., independent of model selection). Although it is important to acknowledge potential limitations, arguably the simplicity of the approaches taken in the present study is a strength: even with an idealized tissue model ECG changes consistent with increased proarrhythmic risk were seen. Consistent with our findings, in the period since original submission of this study, an independent multiscale heart modelling study has been published that found simulation of combined hydroxychloroquine and AZM to produce greater QT prolongation than HCQ alone [35]. It also reported that AZM lowered the threshold for ventricular arrhythmia with HCQ [35]. When the data from all simulations are considered collectively, this study provides clear insight into cardiac effects of high AZM concentrations, such as those that may occur with tissue AZM accumulation. Such conditions can lead to QT interval prolongation and dispersion of ventricular repolarization – electrophysiological changes that predispose towards cardiac arrhythmia.

Declaration of competing interest

The authors declare that they have no known competing financial interests or personal relationships that could have appeared to influence the work reported in this paper.

Acknowledgements

This work was supported by grants from EPSRC (United Kingdom) (EP/J00958X/1 and EP/I029826/1).

Appendix A. Supplementary data

Supplementary data to this article can be found online at https://doi.org/10.1016/j.bbrep.2021.101043.

References

[1] A.H. Bakheit, B.M. Al-Hadiya, A.A. bd-Elgalil, Azithromycin, Profiles Drug. Subst. Excip. Relat. Methodol. 39 (2014) 1–40.
[2] R. Choudhary, A.K. Sharma, R. Choudhary, Potential use of hydroxychloroquine, ivermectin and azithromycin drugs in fighting COVID-19: trends, scope and relevance, New Microb. New Infect. (2020 Apr 22) 100684.
[3] P. Gautret, J.C. Lagier, P. Parola, V.T. Hoang, L. Meddeb, M. Mailhe, et al., Hydroxychloroquine and azithromycin as a treatment of COVID-19: results of an open-label non-randomized clinical trial, Int. J. Antimicrob. Agents (2020 Mar 20) 105949.
[4] M. Million, J.C. Lagier, P. Gautret, P. Colson, P.E. Fournier, S. Amrane, et al., Early treatment of COVID-19 patients with hydroxychloroquine and azithromycin: a retrospective analysis of 1061 cases in Marseille, France, Trav. Med. Infect. Dis. (2020 May 5) 101738.
[5] J.F. Poschet, E.A. Perkett, G.S. Timmins, V. Deretic, Azithromycin and ciprofloxacin have a chloroquine-like effect on respiratory epithelial cells, bioRxiv, https://doi.org/10.1101/2020.03.29.008631, 2020, 1-21.
[6] A. Carpenter, O.J. Chambers, A. El Harchi, R. Bond, O. Hanington, S.C. Harmer, et al., COVID-19 management and arrhythmia: risks and challenges for clinicians treating patients affected by SARS-CoV-2, Front. Cardiovasc. Med. 7 (2020) 85.
[7] A. Cavalcanti, et al., Hydroxychloroquine with or without Azithromycin in Mild-to-Moderate Covid-19, N Engl J Med 383 (2020) 2041–2052, https://doi.org/10.1056/NEJMoa2019014, 6.
[8] R.C. Owens Jr., T.D. Nolin, Antimicrobial-associated QT interval prolongation: pointes of interest, Clin. Infect. Dis. 43 (12) (2006 Dec 15) 1603–1611.
[9] J.C. Hancox, M.J. McPate, A. El Harchi, Y.H. Zhang, The hERG potassium channel and hERG screening for drug-induced torsades de pointes, Pharmacol. Therapeut. 119 (2008) 118–132.
[10] M.B. Thomsen, J.D. Beekman, N.J. Attevelt, A. Takahara, A. Sugiyama, K. Chiba, et al., No proarrhythmic properties of the antibiotics Moxifloxacin or Azithromycin in anaesthetized dogs with chronic-AV block, Br. J. Pharmacol. 149 (8) (2006 Dec) 1039–1048.
[11] P. Milberg, L. Eckardt, H.J. Bruns, J. Biertz, S. Ramtin, N. Reinsch, et al., Divergent proarrhythmic potential of macrolide antibiotics despite similar QT prolongation: fast phase 3 repolarization prevents early afterdepolarizations and torsade de pointes, J. Pharmacol. Exp. Therapeut. 303 (1) (2002 Oct) 218–225.
[12] W.A. Ray, K.T. Murray, K. Hall, P.G. Arbogast, C.M. Stein, Azithromycin and the risk of cardiovascular death, N. Engl. J. Med. 366 (20) (2012 May 17) 1881–1890.
[13] J.C. Hancox, M. Hasnain, W.V. Vieweg, E. Breden-Crouse, A. Baranchuk, Azithromycin, cardiovascular risks, QTc interval prolongation, torsade de pointes, and regulatory issues: a narrative review based on the study of case reports, Ther. Adv. Infect. Dis. 1 (2013) 155–165.
[14] M.H. Kim, C. Berkowitz, R.G. Trohman, Polymorphic ventricular tachycardia with a normal QT interval following azithromycin, Pacing Clin. Electrophysiol. 28 (11) (2005 Nov) 1221–1222.
[15] Z. Yang, J.K. Prinsen, K.R. Bersell, W. Shen, L. Yermalitskaya, T. Sidorova, et al., Azithromycin causes a novel proarrhythmic syndrome, Circ. Arrhythm Electrophysiol. 10 (4) (2017 Apr), e003560.
[16] J.M. Nerbonne, C.G. Nichols, T.L. Schwarz, D. Escande, Genetic manipulation of cardiac K^+ channel function in mice: what have we learned, and where do we go from here? Circ. Res. 89 (11) (2001 Nov 23) 944–956.
[17] T. O'Hara, L. Virag, A. Varro, Y. Rudy, Simulation of the undiseased human cardiac ventricular action potential: model formulation and experimental validation, PLoS Comput. Biol. 7 (5) (2011 May), e1002061.
[18] D.G. Whittaker, H. Ni, A.P. Benson, J.C. Hancox, H. Zhang, Computational analysis of the mode of action of disopyramide and quinidine on hERG-linked short QT syndrome in human ventricles, Front. Physiol. 8 (2017) 759.
[19] C.H. Luo, Y. Rudy, A dynamic model of the cardiac ventricular action potential. I: simulations of ionic currents and concentration changes, Circ. Res. 74 (1994) 1071–1096.
[20] I. Adeniran, M.J. McPate, H.J. Witchel, J.C. Hancox, H. Zhang, Increased vulnerability of human ventricle to re-entrant excitation in hERG-linked variant 1 short QT syndrome, PLoS Comput. Biol. 7 (12) (2011 Dec), e1002313.

[21] J. Tomek, A. Bueno-Orovio, E. Passini, X. Zhou, Development, calibration, and validation of a novel human ventricular myocyte model in health, disease, and drug block, eLife 8 (2019), e48890.
[22] L.M. Hondeghem, L. Carlsson, G. Duker, Instability and triangulation of the action potential predict serious proarrhythmia, but action potential duration prolongation is antiarrhythmic, Circulation 103 (2001) 2004–2013.
[23] M. Yamaguchi, M. Shimizu, H. Ino, H. Terai, K. Uchiyama, K. Oe, et al., T wave peak-to-end interval and QT dispersion in acquired long QT syndrome: a new index for arrhythmogenicity, Clin. Sci. (Lond.) 105 (6) (2003 Dec) 671–676.
[24] B.H. Huang, C.H. Wu, C.P. Hsia, C.C. Yin, Azithromycin-induced torsade de pointes, Pacing Clin. Electrophysiol. 30 (12) (2007 Dec) 1579–1582.
[25] B.C. Hsia, N. Greige, J.A. Quiroz, A.S. Khokhar, J. Daily, B.L. Di, et al., QT prolongation in a diverse, urban population of COVID-19 patients treated with hydroxychloroquine, chloroquine, or azithromycin, J. Intervent. Card Electrophysiol. 11 (2020) 1–9.
[26] L.S. Nguyen, C. Dolladille, M.D. Drici, C. Fenioux, J. Alexandre, J.P. Mira, et al., Cardiovascular toxicities associated with hydroxychloroquine and azithromycin: an analysis of the World health organization pharmacovigilance database, Circulation 142 (3) (2020 Jul 21) 303–305.
[27] M. Zhang, et al., Electrophysiologic studies on the risks and potential mechanism underlying the proarrhythmic nature of azithromycin, Cardiovasc. Toxicol. 17 (4) (2017) 434–440.
[28] H. Ohara, et al., Azithromycin can prolong QT interval and suppress ventricular contraction, but will not induce torsade de Pointes, Cardiovasc. Toxicol. 15 (3) (2015) 232–240.
[29] J.A. Sanchez-Chapula, T. Ferrer, R.A. Navarro-Polanco, M.C. Sanguinetti, Voltage-dependent profile of human ether-a-go-go-related gene channel block is influenced by a single residue in the S6 transmembrane domain, Mol. Pharmacol. c63 (5) (2003) 1051–1058.
[30] M. Traebert, B. Dumotier, L. Meister, P. Hoffmann, M. Dominguez-Estevez, W. Suter, Inhibition of hERG K^+ currents by antimalarial drugs in stably transfected HEK293 cells, Eur. J. Pharmacol. 484 (1) (2004) 41–48, 19.
[31] L. Moschini, M. Loffi, V. Regazzoni, T.G. Di, E. Gherbesi, G.B. Danzi, Heart Ves. 16 (2020) 1–6.
[32] P. Matzneller, S. Krasniqi, M. Kinzig, F. Sorgel, S. Huttner, E. Lackner, et al., Blood, tissue, and intracellular concentrations of azithromycin during and after end of therapy, Antimicrob. Agents Chemother. 57 (4) (2013 Apr) 1736–1742.
[33] G.A. Gintant, J.T. Limberis, J.S. McDermott, C.D. Wegner, B.F. Cox, The canine Purkinje fiber: an in vitro model system for acquired long QT syndrome and drug-induced arrhythmogenesis, J. Cardiovasc. Pharmacol. 37 (5) (2001 May) 607–618.
[34] F.G. Araujo, R.M. Shepard, J.S. Remington, In vivo activity of the macrolide antibiotics azithromycin, roxithromycin and spiramycin against Toxoplasma gondii, Eur. J. Clin. Microbiol. Infect. Dis. 10 (6) (1991 Jun) 519–524.
[35] J.-I. Okada, T. Yoshinaga, T. Washio, K. Sawada, S. Sugiura, T. Hisada, Chloroquine and hydroxychloroquine provoke arrhythmias at concentrations higher than those clinically used to treat COVID-19: a simulation study, Clin. Transl. Sci. (2021) 1–9 (PMID 33404133).